Journal of Applied Polymer Science

Experimental and theoretical investigation of sound transmission loss for polycarbonate, poly(methyl methacrylate), and glass

Seyed Mohammad Sabet, Abdolreza Ohadi
Acoustics Research Laboratory, Department of Mechanical Engineering, Amirkabir University of Technology (Tehran Polytechnic), Tehran, Iran
Correspondence to: A.R. Ohadi (E-mail: a_r_ohadi@aut.ac.ir)

ABSTRACT: In this study, the effects of the soundproofing properties of polycarbonate (PC), poly(methyl methacrylate) (PMMA), and glass were investigated. We fabricated the specimens into 3 mm thick sheets by direct hot compression molding as a monolithic sample and also by gluing three thin sheets together into a multilayer. Sound transmission loss (STL) was measured by an impedance tube over the frequency range 63–1600 Hz. The results indicate that because of the close density, the STLs for PC and PMMA were almost the same above 1200 Hz. Also, PMMA had a greater STL than PC in the range 63–300 Hz. In a comparison of the monolithic and multilayered samples, we demonstrated that the epoxy-based adhesive interlayers had more efficient bonding than the silicone-based ones. The multilayered polymer/silicone specimens showed a sharp drop in the STL values compared to the monolithic samples. However, the multilayered polymer/epoxy specimens revealed similar behavior to the monolithic polymers. © 2015 Wiley Periodicals, Inc. J. Appl. Polym. Sci. **2016**, *133*, 42988.

KEYWORDS: adhesives; polycarbonates; properties and characterization

Received 10 August 2015; accepted 27 September 2015
DOI: 10.1002/app.42988

INTRODUCTION

In the study of sound transmission through structures, the utilization of sound isolation materials is among the most common technique in the area of passive noise control. Soundproofing materials cause a large change in the acoustic impedance in the transmission path to reduce ambient noise. Many studies have been carried out on the basis of the experimental and theoretical aspects of sound transmission loss (STL).[1–6] Some of these studies have focused on the different kinds of multilayered structures, such as double-leaf systems with an air space or sandwich panels.[7–10] On the other hand, many experiments have been done to investigate the soundproofing properties of the various kinds of industrial materials. Zhao *et al.*[11] worked on the sound insulation properties of three composite panels: wood-waste tire rubber composite panels (WRCPs), commercial compound wooden floorboards, and wood-based particleboard. Their analysis showed that the WRCPs had more soundproofing effects than the others. They also improved STL for the WRCPs by increasing the rubber crumb content and polymeric methylene diphenyl diisocyanate adhesive level used in the composite.

In the last 2 decades, scientists have been interested in the behavior of advanced new materials as sound-isolating substances. Ng and Hui[12] used a new honeycomb core design to increase the stiffness of a panel and improve the noise transmission loss (TL) at low frequencies. They also introduced a model to predict the STL of honeycomb panels. Mahjoob *et al.*[13] investigated the effect of a magnetic field on the STL of smart multilayered panels and also developed an acoustic model for a multilayered panel containing magnetorheological fluid. They found a good correlation between the model and experiments at low frequency and discussed the discrepancy at higher frequencies. Also, functionally graded material (FGM), introduced in recent years, is among the newest materials that have drawn scientists' attention. Chandra *et al.*[14] analytically studied the vibroacoustics of FGM plates with a simple first-order shear deformation theory. They compared the soundproofing properties and radiation efficiency of metal-rich and ceramic-rich FGM plates at lower (0–500 Hz) and higher frequencies. Huang and Nutt[15] studied sound reflection and transmission through unbounded FGM panels by an analytical approach. In addition to these new materials, some studies have been carried out to improve the isolation performance via various absorbing techniques. Mu *et al.*[16] investigated the influence of installing a microperforated panel on single and multilayer windows. They found that the perforation of a leaf of double- or triple-glass window improved the STL degradation; this was caused by mass–air–mass resonance. Bravo *et al.*[17] established a fully coupled modal approach to determine the absorption and transmission coefficients of finite-sized microperforated panels backed by an air

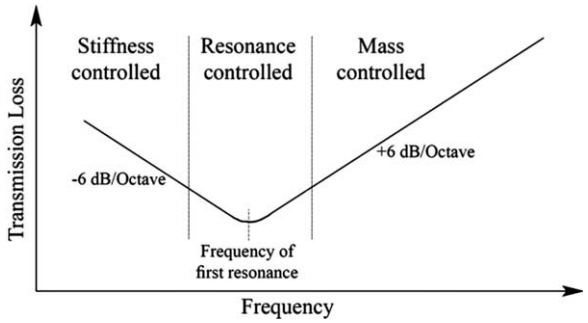

Figure 1. Typical scheme of normal-incidence STL for a single panel.

cavity and a thin plate. They validated the model by measuring the transmission and absorption properties of a baffled microperforated panel–cavity–panel layout. Also, a comparison was carried out between the model and the literature's theoretical results on infinite partition models. They obtained the same Helmholtz resonance frequency for both a microperforated panel–cavity–panel partition and a rigidly backed microperforated panel absorber.

In the case of transparent materials, many types of glass panels are available; however, because of the brittle nature of the glass, transparent polymer materials are the best choice for this purpose. Polycarbonate (PC) and poly(methyl methacrylate) (PMMA) are the most suitable substitutes for glass as transparent materials. Considerable research has been reported on the effects of different kinds of soundproofing glass panels[18–20]; also, there have been many works published on various aspects of PC and PMMA,[21–23] but to our knowledge, no reports have focused on PC's and PMMA's sound isolation properties. Therefore, in this article, we present the theoretical and experimental sound transmitting behavior for these two polymer materials.

In addition, to improve the TL through the addition of extra layers on a partition and make a solid multilayered structure, it is important to determine the changes occurring because of the increasing panel thickness. Therefore; in addition to the aims pursued previously, the influence of adhesive interlayers was also investigated through a comparison of monolithic and multilayered panels both for PC and PMMA.

THEORETICAL FORMULATION

There are many methods for predicting the panel's STL under different conditions. In the case of single panels, STL is dominated by some main physical factors, including the surface mass, bending stiffness, dimensions, loss factor (η), and sound incident angle.[24] Figure 1 represents a typical normal incidence TL scheme for a single panel, with various characteristic frequency ranges.

To calculate the STL, the first resonance frequency (ω_0) needs to be defined. Fahy and Gardonio[25] introduced the frequency of the first resonance for a rigid panel with flexible supports as follows:

$$\omega_0 = \sqrt{k_s/m} \tag{1}$$

where k_s is the stiffness per unit area for the panel's support and the surface density (m) can be replaced by ρh (where ρ and h are the density and thickness of the panel, respectively). The natural frequencies for a circular flexible plate ($\omega_{m,n}$'s) are as follows:

$$\omega_{m,n} = \frac{(\lambda r)^2_{m,n}}{r^2}\sqrt{\frac{D}{\rho h}} \quad m, n = 0, 1, 2, \ldots \tag{2}$$

where r is the radius and $(\lambda r)_{m,n}$ is obtained from the plate's characteristic equation. Also, D is the plate's bending stiffness and is given by

$$D = \frac{Eh^3}{12(1-\nu^2)} \tag{3}$$

where E is the elastic modulus and ν is Poisson's ratio.

With the first mode of vibration (i.e., $m = n = 0$), the equivalent k_s could be derived through a comparison of eqs. (1) and (2) as follows:

$$k_s = \frac{(\lambda r)^4}{r^4} D \tag{4}$$

It is clear that the TL is not only a property of material and geometrical parameters but is also strongly dependent on the mounting conditions. In this study, three different cases were considered to investigate the sample's mounting conditions in the impedance tube. For simply supported and fixed boundary conditions (BCs), equivalent k_s values can be derived by the substitution of values of λr of 2.108 and 3.196 in eq. (4), respectively. To seal and hold the samples in position, a rubbery sealant was used to prevent any sound leakage; under such conditions, specimens showed restrictive movement along the tube; this caused BC to show a behavior between simply supported and fixed edge. Through the adjustment of the theoretical and experimental resonance frequencies, a value of λr of 2.62 was obtained to model this elastic BC. This adjustment is discussed in detail later.

Norton and Karczub[26] introduced a general model for STL through a single panel as follows:

$$\mathrm{TL} = 10\log_{10}\left|1 + \frac{(Z'_m + Z'_r)\cos\theta}{2\rho_0 c}\right|^2 \tag{5}$$

where Z'_m and Z'_r are the mechanical and radiation impedances per unit area, respectively; $\rho_0 c$ is the characteristic impedance of the medium; and θ is the sound incident angle. In the impedance tube test method, with the existence of air on both sides of the specimen as the fluid medium and also because of the small size of the sample area, acoustic radiation could be neglected. The mechanical impedance of a bounded panel with a uniform distribution of mass, stiffness, and damping is given as follows:

$$Z'_m = C_v + i(m\omega - k_s/\omega) \tag{6}$$

where ω is the frequency (rad/s) and the viscous damping (C_v) can be replaced by $\eta\omega m$.[26] Thus, through the substitution of eq. (6) into eq. (5) and with normal incident (i.e., $\theta = 0$), STL becomes

$$\mathrm{TL} = 10\log_{10}\left[\left(1 + \frac{\eta\omega m}{2\rho_0 c}\right)^2 + \left(\frac{m\omega - k_s/\omega}{2\rho_0 c}\right)^2\right] \tag{7}$$

Table I. Physical and Mechanical Properties of PC and PMMA

Property	PC (C-206)	PMMA (CM-205)
Density (g/cm^3)	1.23	1.19
Melt flow index (g/10 min)	7.1–10	14.35
Modulus of elasticity (MPa)	2600	3900
Loss factor	0.04	0.086
Poisson's ratio	0.37	0.37

To calculate the TL values as a function of the frequency, the parameters η, m, and $\rho_0 c$ in eq. (7) could be easily obtained from the physical and mechanical properties of the panel and the medium (in this study, air). Also, k_s was replaced with equivalent stiffness from eq. (4); thereby, the TL values were calculated as a function of the frequency. Depending on the use of different equivalent stiffnesses, the corresponding TLs were determined for different BCs.

EXPERIMENTAL

Materials

The polymer specimens were constructed with PC (C-206) obtained from Khouzestan Petrochemical Co. (Iran) and PMMA (Acryrex CM-205) obtained from Chi Mei Corp. (Taiwan). Table I shows the properties of the polymer materials used.

Specimen Preparation

Two different kinds of specimens were constructed. First, sheets 3 mm thick were fabricated by direct hot compression molding as a monolithic material, and second, three 1-mm sheets were constructed via hot compression molding and then glued onto each other as a multilayer with the same thickness as monolithic sheets. These two methods were performed for both polymer materials, that is, PC and PMMA.

To mold the sheets, PC granules were heated in an oven for about 6 h at 110°C to remove any moisture, and the molding process were performed at 300°C with a hot press. To prevent shrinking defects, the hot press was left to cool gradually to room temperature. Also, the PMMA samples were constructed in the same manner; the drying process for PMMA was accomplished in about 4 h at 90°C, and the hot compression-molding process was done at 240°C. For the multilayered samples, the three 1-mm layers were bonded together by two different kinds of adhesives under pressure to reach a very thin bonding line interlayer. Epoxy- and silicone-based adhesives were used for multilayered specimens. The prepared sheets were laser-cut to a circle shape per impedance tube requirements with a diameter of 10 cm.

Test Method

Dynamic mechanical analysis (DMA) was carried out to measure the mechanical properties of the polymer materials with TTDMA from Triton Technology Co. (United Kingdom). An impedance tube method per ASTM E 2611-09 was used to measure the normal TL for the specimens. The impedance tube (SW 422) from BSWA Technology Co. (China) was used in a frequency range of 63–1600 Hz.

In general, for a finite panel, the mounting conditions will strongly affect STL. In the impedance tube test method, the specimen may be freely suspended with a dense flexible seal or some other method of mounting. Clearly, a small opening around the sample's edge will lead to a significant effect on the TL calculations. Therefore, in this study, a rubbery sealant was used to hold the samples in position and prevent any sound leakage from peripheral cracks or gaps. Figure 2 shows the impedance tube setup, the rubbery sealant, and the specimens with and without sealant used.

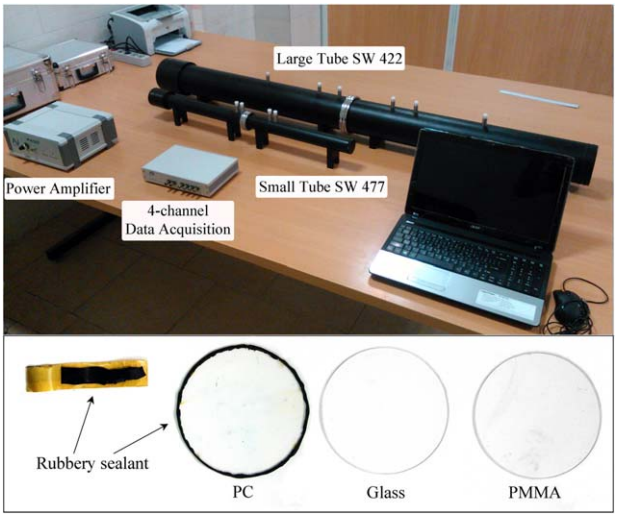

Figure 2. Impedance tube setup and specimens. [Color figure can be viewed in the online issue, which is available at wileyonlinelibrary.com.]

RESULTS AND DISCUSSION

In this study, two different subjects were investigated. First, a comparison was made between the soundproofing properties of PC, PMMA, and glass. Also, the theoretical and experimental results are presented for both polymer materials. Second, the multilayered specimens were compared with monolithic ones for both PC and PMMA, and the influence of epoxy- and silicone-based adhesive interlayers on STL were assessed.

DMA

Figure 3 shows the storage modulus and phase angle (or loss factor) versus frequency for both PC and PMMA. It indicates a similar response for both materials with PMMA showing a greater storage modulus and also a greater phase angle, especially at low frequencies (i.e., 0–150 Hz), than PC. Furthermore, the study of Figure 3 revealed two distinct regions for the storage modulus and phase angle for the both polymer materials, that is, a plateau region signifying an elastic response and a sharp drop. In general, the dynamic mechanical test method contains two distinct time domains that need to be studied, namely, the time of excitation and the time of material's response. At low frequencies, there was enough time for material response, so the material retained its elastic behavior. As shown in Figure 3, the elastic range (i.e., 0–150 Hz), in which the material properties are constant, was easily observed. However, at high frequencies, excitation was faster than the material's response, and material softening occurred. This phenomenon caused a decrease in the storage modulus and an increase in the damping properties. Therefore, as expected the storage modulus was reduced as the frequency increased over the

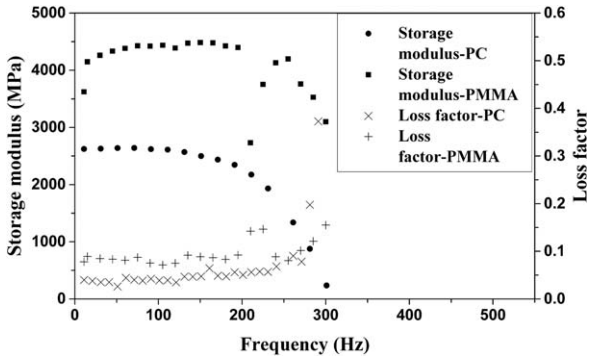

Figure 3. DMA for both monolithic PC and PMMA.

range 150–300 Hz, but this behavior was reversed for the phase angle.

We noted that the specimens in the impedance tube are excited by acoustics waves and they vibrate elastically. Therefore, for the theoretical studies of STL, mechanical properties at elastic region (i.e., DMA mechanical properties at low frequencies) are used.

Comparing STL for Monolithic PC, PMMA, and Glass

STL values for the monolithic PC, PMMA, and glass are depicted in Figure 4. As shown, in the stiffness control region (i.e., 63–300 Hz), PMMA had a greater STL value than PC; this was about 4.7 dB on average. This behavior was expected because PMMA had a higher elastic modulus compared to PC, and this caused a higher stiffness. Table I shows that PC and PMMA had a very close density; this resulted in almost the same STL in the mass control region and explained why PC and PMMA's STL got closer to each other in the range 1000–1600 Hz.

In the range 300–1000 Hz, the first resonance frequency occurred both for PC and PMMA at 526 and 644 Hz, respectively. In this region, all of the stiffness, density, and structural loss factor values of the polymer materials dominated the STL values; therefore, as shown in Figure 4, PMMA had a greater STL than PC from 300–600 Hz, and this was reversed from 600 to 1000 Hz. That is, the STL value for PC was higher than that of PMMA.

On the other hand, a comparison of glass with both PC and PMMA indicated that the glass had higher stiffness than the other two; this was due to the high elastic modulus for glass

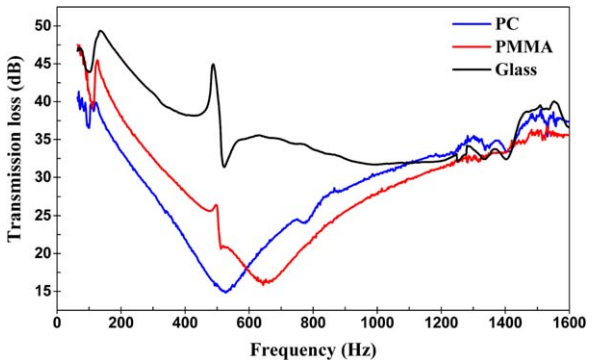

Figure 4. Experimental STL values for glass and monolithic PC and PMMA. [Color figure can be viewed in the online issue, which is available at wileyonlinelibrary.com.]

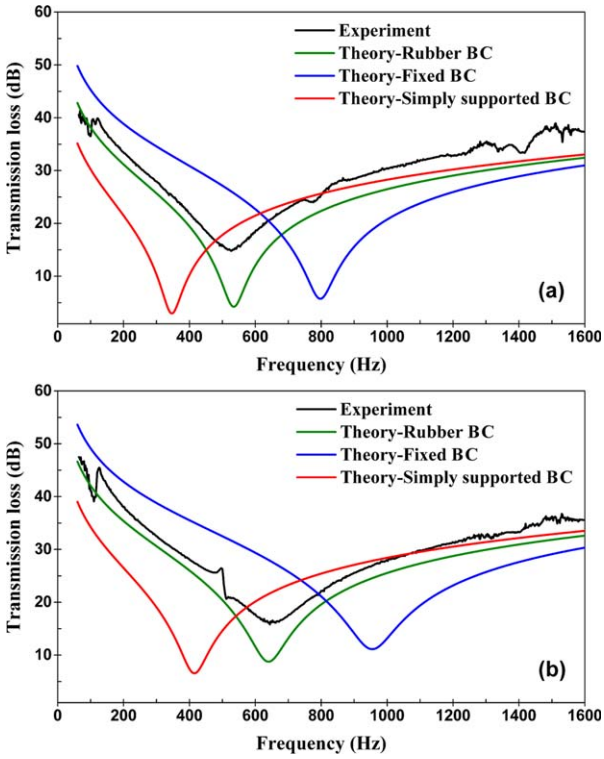

Figure 5. Experimental and theoretical results for (a) PC and (b) PMMA. [Color figure can be viewed in the online issue, which is available at wileyonlinelibrary.com.]

(70 GPa). This resulted in a significantly higher STL compared to those of PC and PMMA over the frequency range 63–800 Hz. Because of the higher elastic modulus of the glass, the first resonance frequency occurred around 1100 Hz; therefore, its STL curve decreased until it reached the first resonance.

We also observed from Figure 4 that there were two strange peaks near 500 Hz for both glass's and PMMA's curves. This change may not have been associated with the material's sound-isolating behavior, but it was attributed to the sealant and mounting conditions. The rubbery sealant let the specimen have a rigid body motion along with the tube length; this may have been related to the changes in the system's degrees of freedom and resulted in the appearance of two peaks in the STL diagram. We expected that the same thing happened for the PC curve, but here, it coincided with the first resonance frequency and was not observed.

In this study, as mentioned before, three cases were considered for the investigation and modeling of the sample's mounting conditions in the impedance tube. According to eq. (4), equivalent k_s values were obtained with λr values of 2.108 for a simply supported BC and 3.196 for a fixed BC. The substitution of this equivalent stiffness into eq. (7) and with the geometrical and mechanical properties of the specimens, the theoretical TL values were calculated as function of the frequency.

Figure 5(a,b) shows the theoretical and experimental results for PC and PMMA. Clearly, there was a considerable difference in the frequencies of the first resonance between the experimental results and these two theoretical results (i.e., the curves of the

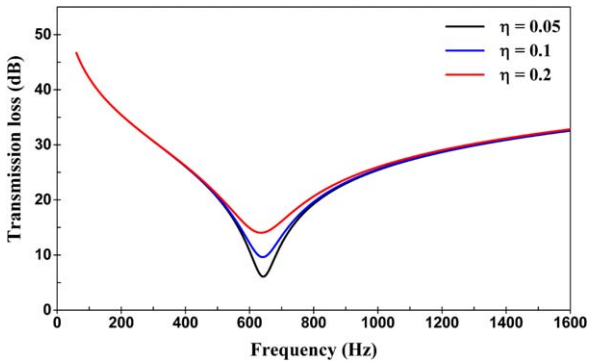

Figure 6. Theoretical curves for different loss factor values. [Color figure can be viewed in the online issue, which is available at wileyonlinelibrary.com.]

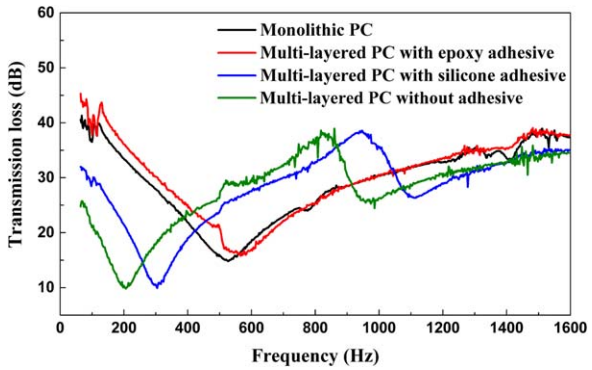

Figure 7. Experimental STL values for monolithic and multilayered PC. [Color figure can be viewed in the online issue, which is available at wileyonlinelibrary.com.]

fixed BC and simply supported BC) for both PC and PMMA. This may have been due to the sample's BC. The specimens were mounted in the impedance tube with a rubbery sealant, so this type of holding could not be modeled as simply supported or fixed; actually, the rigidity of the test BC was something between the two. Therefore, to compare the theory with the experimental results, the equivalent stiffness was adjusted by the selection of an λr value of 2.62, so the theoretical resonance frequency was matched with the experimental one. This case is illustrated in Figure 5(a,b) as the rubber BC curve.

Although eq. (7) presents the general behavior of the system, there were differences in the STL values from the theory and experimental data; this was shown in the whole range of frequency (i.e., 63–300 Hz). It was clear that eq. (7) could not properly predict the STL values under these conditions; this may have been due to the simplifying assumptions made. In fact, according to eq. (5), only the first mode of vibration is considered. So, eq. (7) does not include higher modes of the panel. Actually, these theoretical formulations were useful for the approximate prediction of the general behavior of STL, but they could not calculate accurately.

Furthermore, the study of Figure 5(a,b) revealed that there was a significant difference between the prediction and experimental results at resonance frequency (cf., the two theories, rubber BC, and experiment's curves). It is known that at the resonance frequency, the damping characteristics of the system dominated STL. Therefore, such a major difference was attributed to the fact that the rubbery sealant had higher damping properties than both polymer materials; so at this range of frequency, a combination of the rubber and panel's loss factors dominated the TL values. Figure 6 shows theoretical results for three different loss factor values. The increase in STL at resonance is clearly shown as the effect of higher damping.

STL for Monolithic and Multilayered Samples

STL values are presented for monolithic and multilayered PC's specimens in Figure 7. According to this diagram, the frequencies of the first resonances occurred at 200, 300, 550, and 500 Hz for the multilayered PC with no adhesive interlayers (PC/no-ADH), multilayered PC with silicone interlayered adhesives (PC/silicone), PC with epoxy interlayered adhesive (PC/epoxy), and monolithic PC, respectively. Because of the fact that the very thin adhesive interlayers could not affect the density, this change in the first resonance frequency indicated that the bending stiffness for the multilayered PC/epoxy was almost the same as the monolithic one, but the multilayered PC/silicone and PC/no-ADH showed significant decreases in the stiffness. As shown in Figure 7, in the frequency range 63–150 Hz, which was almost the stiffness control region for all four samples, the multilayered PC/epoxy had a very close STL to the monolithic PC, but the multilayered PC/silicone and PC/no-ADH showed a sharp drop in STL compared to monolithic one; these values were about 10 and 18 dB, respectively, on average; this confirmed the changes in the stiffness, as mentioned earlier. We noted that the samples were subjected to a normal incident plane wave in the impedance tube; therefore, the coincidence frequency would not naturally exist. It was clear that the second drop point in the curves of the multilayered PC/silicone and PC/no-ADH corresponded to the multilayered resonance frequencies. Obviously, for PC/epoxy, this point occurred above 1600 Hz.

On the other hand, Figure 8 showed similar curves for the monolithic and multilayered PMMA. As shown here, the multilayered PMMA/epoxy samples had a very close STLs to that of monolithic PMMA, but as before, the multilayered PMMA/silicone and PMMA/no-ADH showed decreases in STL compared to the monolithic one; these were about 5 and 17 dB, respectively, on average in the stiffness control region. This means that the epoxy-based adhesive had a better performance in gluing the polymer

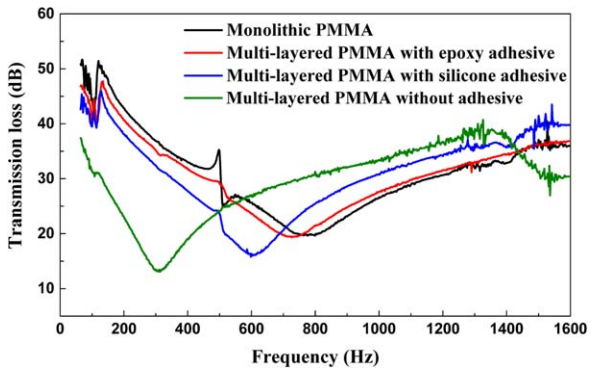

Figure 8. Experimental STL values for monolithic and multilayered PMMA. [Color figure can be viewed in the online issue, which is available at wileyonlinelibrary.com.]

layers compared to the silicone-based adhesive. In the frequency range of 1200–1600 Hz, the STL values for both the monolithic and multilayered PMMA samples with adhesive got closer to each other; this explained that the thin adhesive interlayers had a negligible effect on the specimen's density. Also, it was obvious that the multilayered resonance frequency occurred at 1540 Hz for multilayered PMMA/no-ADH, but for the other multilayered specimens, it occurred at higher frequencies.

Furthermore, a focus on the resonance frequencies shown in Figure 7 demonstrates that the monolithic PC and multilayered PC/epoxy had more TL values at resonance than the other two (i.e., the multilayered PC/silicone and PC/no-ADH). This behavior was also repeated for the PMMA samples, shown in Figure 8. As mentioned earlier, at resonance, the system was damping controlled, so the higher frequency resonance led to a higher corresponding STL. In other words, at resonance, the STL values increased with increasing frequency.

CONCLUSIONS

A comparison between PMMA and PC revealed that PMMA was stiffer than PC; therefore, it had better sound-isolation properties in the stiffness control region; this was about 4.7 dB on average. However, the glass had a higher STL compared to both polymer materials. Our theoretical study indicated that the mounting conditions of the specimens through holding with a rubbery sealant in the impedance tube showed behavior between simply supported and fixed BCs. Also, common theoretical formulations, which include only the first mode of vibration, could not accurately predict the STL values.

Impedance tube tests for the monolithic and multilayered samples demonstrated the influence of very thin adhesive interlayers. The results show that the bonding between the epoxy-based adhesive and the polymer materials (i.e., PC and PMMA) were more efficient than bonding with silicone-based adhesives. Also, we concluded that the thin adhesive interlayers had no significant effect on STL over the frequency range 1200–1600 Hz, which was about the mass control region. Therefore, it is important to select a suitable adhesive with regard to the panel's material in the case of the increase in the panel's thickness through the addition of extra layers.

REFERENCES

1. Pellicier, A.; Trompette, N. *Appl. Acoust.* **2007**, *68*, 1192.
2. Wang, X.; You, F.; Zhang, F. S.; Li, J.; Guo, S. *J. Appl. Polym. Sci.* **2011**, *122*, 1427.
3. Natsuki, T.; Ni, Q.-Q. *Appl. Phys. Lett.* **2014**, *105*, 201907.
4. Oudich, M.; Zhou, X.; Assouar, M. B. *J. Appl. Phys.* **2014**, *116*, 193509.
5. Shimizu, T.; Toyoda, M.; Takahashi, D.; Kawai, Y. *Appl. Acoust.* **2013**, *74*, 1010.
6. Liang, J. Z.; Jiang, X. H. *J. Appl. Polym. Sci.* **2012**, *125*, 676.
7. Vigran, T. *J. Sound Vibr.* **2009**, *325*, 507.
8. Dym, C. L.; Lang, M. A. *J. Acoust. Soc. Am.* **1974**, *56*, 1523.
9. Panneton, R.; Atalla, N. *J. Acoust. Soc. Am.* **1996**, *100*, 346.
10. Sgard, F.; Atalla, N.; Nicolas, J. *J. Acoust. Soc. Am.* **2000**, *108*, 2865.
11. Zhao, J.; Wang, X.-M.; Chang, J.; Yao, Y.; Cui, Q. *Compos. Sci. Technol.* **2010**, *70*, 2033.
12. Ng, C.; Hui, C. *Appl. Acoust.* **2008**, *69*, 293.
13. Mahjoob, M. J.; Mohammadi, N.; Malakooti, S. *Appl. Acoust.* **2012**, *73*, 614.
14. Chandra, N.; Raja, S.; Gopal, K. N. *J. Sound Vibr.* **2014**, *333*, 5786.
15. Huang, C.; Nutt, S. *J. Sound Vibr.* **2011**, *330*, 1153.
16. Mu, R. L.; Toyoda, M.; Takahashi, D. *Acoust. Sci. Technol.* **2011**, *32*, 79.
17. Bravo, T.; Maury, C.; Pinhède, C. *J. Acoust. Soc. Am.* **2012**, *131*, 3853.
18. Tadeu, A. J.; Mateus, D. M. *Appl. Acoust.* **2001**, *62*, 307.
19. Quirt, J. *J. Acoust. Soc. Am.* **1982**, *72*, 834.
20. Quirt, J. *J. Acoust. Soc. Am.* **1983**, *74*, 534.
21. Duquesne, S.; Jimenez, M.; Bourbigot, S. *J. Appl. Polym. Sci.* **2014**, *131*, 39566. doi: 10.1002/app.39566.
22. Fan, C. F.; Cagin, T.; Chen, Z. M.; Smith, K. A. *Macromolecules* **1994**, *27*, 2383.
23. Torikai, A.; Ohno, M.; Fueki, K. *J. Appl. Polym. Sci.* **1990**, *41*, 1023.
24. Praščević, M.; Cvetković, D.; Mihajlov, D. *Facta Univ. Ser. Arch. Civil Eng.* **2012**, *10*, 155.
25. Fahy, F. J.; Gardonio, P. Sound and Structural Vibration: Radiation, Transmission and Response; Academic: Waltham, MA, **2007**.
26. Norton, M. P.; Karczub, D. G. Fundamentals of Noise and Vibration Analysis for Engineers; Cambridge University Press: Cambridge, United Kingdom, **2003**.